

Received: 2016.06.18  
Accepted: 2016.07.25  
Published: 2017.03.01

# Increased Local Sympathetic Nerve Activity During Pathogenesis of Ventricular Arrhythmias Originating from the Right Ventricular Outflow Tract

Authors' Contribution:  
Study Design A  
Data Collection B  
Statistical Analysis C  
Data Interpretation D  
Manuscript Preparation E  
Literature Search F  
Funds Collection G

ABDEF **Zefeng Wang**  
BC **Huikuan Gao**  
BF **Ruiqing Dong**  
BC **Can Zhao**  
BC **Tianyu Yu**  
BC **Lu Yang**  
AD **Hui Peng**  
ADF **Yongquan Wu**

Department of Cardiology, Beijing Friendship Hospital, Capital Medical University, Beijing, P.R. China

**Corresponding Author:** Yongquan Wu, e-mail: wuyongquan67@163.com  
**Source of support:** Departmental sources

**Background:** The contribution of local sympathetic nerves to ventricular arrhythmia (VA) originating from the right ventricular outflow tract (RVOT) has not been elucidated. This study used a canine model to investigate the anatomical changes of the RVOT associated with VA, and the distribution of local sympathetic nerves.





**Material/Methods:** The RVOT-VA canine model (6 dogs) was induced with a circular catheter and high-frequency stimulation (100 Hz) in the middle of the pulmonary artery trunk. Six dogs who were not given stimulation served as the control group. The serum levels of neurotransmitters, the extent of myocardial extension, and the sympathetic nerve density of the RVOT were also analyzed.

**Results:** Ventricular arrhythmias, including premature ventricular contractions, were induced in the experimental group after high-frequency stimulation. Dogs from the RVOT-VA group showed enhanced myocardial extension and sympathetic nerve density in the septal wall as compared with those of the free wall of the RVOT. In the RVOT-VA dogs, serum norepinephrine and neuropeptide Y and the sympathetic nerve density were significantly higher compared with the control group.

**Conclusions:** Stimulation of the pulmonary artery could activate local sympathetic nerves and enhance myocardial extension, which may be the foundation of RVOT-VA. The RVOT voltage transitional zone positively correlated with myocardial extension, which may serve as an important target for the radiofrequency catheter ablation of RVOT-VA clinically.

**MeSH Keywords:** **Arrhythmias, Cardiac • Autonomic Nervous System • Cardiac Electrophysiology**

**Full-text PDF:** <http://www.medscimonit.com/abstract/index/idArt/900143>

 2049  1  6  21



## Background

Clinical studies have shown that idiopathic ventricular arrhythmia (VA) originating from the right ventricular outflow tract (RVOT), or RVOT-VA, is the most important category of VA, accounting for 70% to 85% of VAs [1]. RVOT-VA is characterized in a 12-lead electrocardiography (ECG) as a left bundle branch block with an inferior axis in the frontal plane [2–4]. For the pharmacological and electrophysiological treatment of arrhythmias, an understanding of the pathogenesis of RVOT-VA is fundamental. It has been reported that activation of sympathetic tone, and the attenuation of parasympathetic nerve activity, may be involved in the pathogenesis of idiopathic VA [5], and these changes seem to occur before the onset of the VA [6–8]. However, the activities of the sympathetic nerves of the myocardium during the development of RVOT-VA have not been comprehensively evaluated.

Studies in animal models have confirmed that high-frequency stimulation in the pulmonary artery can induce a left bundle branch block with inferior axis premature ventricular contractions or ventricular tachycardia [9]. This is similar to the development of RVOT-VA in human patients. However, aggressive conventional stimulation is sometimes not adequate for the induction of VAs [10]. Instead, stimulation of the proximal pulmonary artery can successfully induce VAs, and subsequently lead to catheter ablation therapy for the VAs. Moreover, ventricular myocardial extensions into the pulmonary artery beyond the pulmonary valve have been observed by Hasdemir et al. [11]. These anatomic features of incomplete myocardial regression may suggest the presence of a myocardial sleeve in the main stem of the pulmonary artery that is connected to the rest of the related ventricles. However, these myocardial extensions into the pulmonary artery seem to be ubiquitous in humans [12], and frequently serve as origins of presumed RVOT arrhythmias. Possible changes in the activities of local sympathetic nerves during the pathogenesis of VA, originating from the RVOT, have not been fully determined.

In this study, we used a canine model of sympathetic nerve-induced RVOT-VA to evaluate the anatomical characteristics of the RVOT and the myocardial distribution of sympathetic nerves in RVOT-VA. Also in this model, we investigated an association between RVOT myocardial extension and the voltage transition zone in the pathogenesis of VA. Results of our study may improve the understanding of the role of local sympathetic nerves in the pathogenesis of RVOT-VA, and provide some new evidence for the ablation target region for RVOT-VA clinically.

## Material and Methods

The Institutional Animal Care and Use Committee at Capital Medical University reviewed and approved the study protocol before the experiment was conducted.

### Establishment of a model of RVOT-VA mediated by sympathetic nerves

Twelve adult beagle dogs were anesthetized using sodium pentobarbital. A 20-pole circular catheter (Lasso) (Biosense Webster, Diamond Bar, CA, USA) was introduced into the right femoral vein in all dogs and then positioned in the pulmonary artery with the help of a fluoroscope, until all the ventricular ECG waves disappeared. Recordings of myocardial potentials were achieved from each of the lasso electrode pairs. All tracings from the electrode catheters were amplified and digitally recorded with an electrophysiology workstation (CardioLab, GE, Freiburg, Germany). The surface ECG filter settings were 0.01–250 Hz, whereas the bipolar electrograms were filtered at 30–250 Hz. High-frequency stimulation at 100 Hz (2-ms pulse duration) was applied to the catheter in 6 dogs randomly assigned as the experimental group, while the remaining 6 dogs served as the control group without high-frequency stimulation (Figure 1). The successful induction of VA in the canine RVOT-VA model was confirmed on ECG by the appearance of the following, based on previous animal studies: left bundle branch block, right axis deviation, and II, III, and aVF lead R one-way wave [9].

### Voltage mapping of the RVOT

Voltage mapping was performed in dogs of both groups under the guidance of a 3-dimensional electroanatomical mapping CARTO system (Biosense Webster, CA, USA) under sinus rhythm. These procedures were achieved by taking about 1000 points and building a 3-dimensional conformation of the canine RVOT. Characteristics of the voltage transition zone of the RVOT from all the dogs were observed and analyzed.

### Serum concentrations of neurotransmitters

Blood samples were taken and collected before and after stimulation of the canine coronary sinus. The serum concentrations of norepinephrine, neuropeptide Y, and acetylcholine were determined with enzyme-linked immunosorbent assay (ELISA) in accordance with the instructions of the manufacturers.

### Canine RVOT muscle extension distribution

After the electrophysiological examination, the dogs were killed and the ventricular outflow myocardium was removed and stained with hematoxylin-eosin (H&E) for subsequent

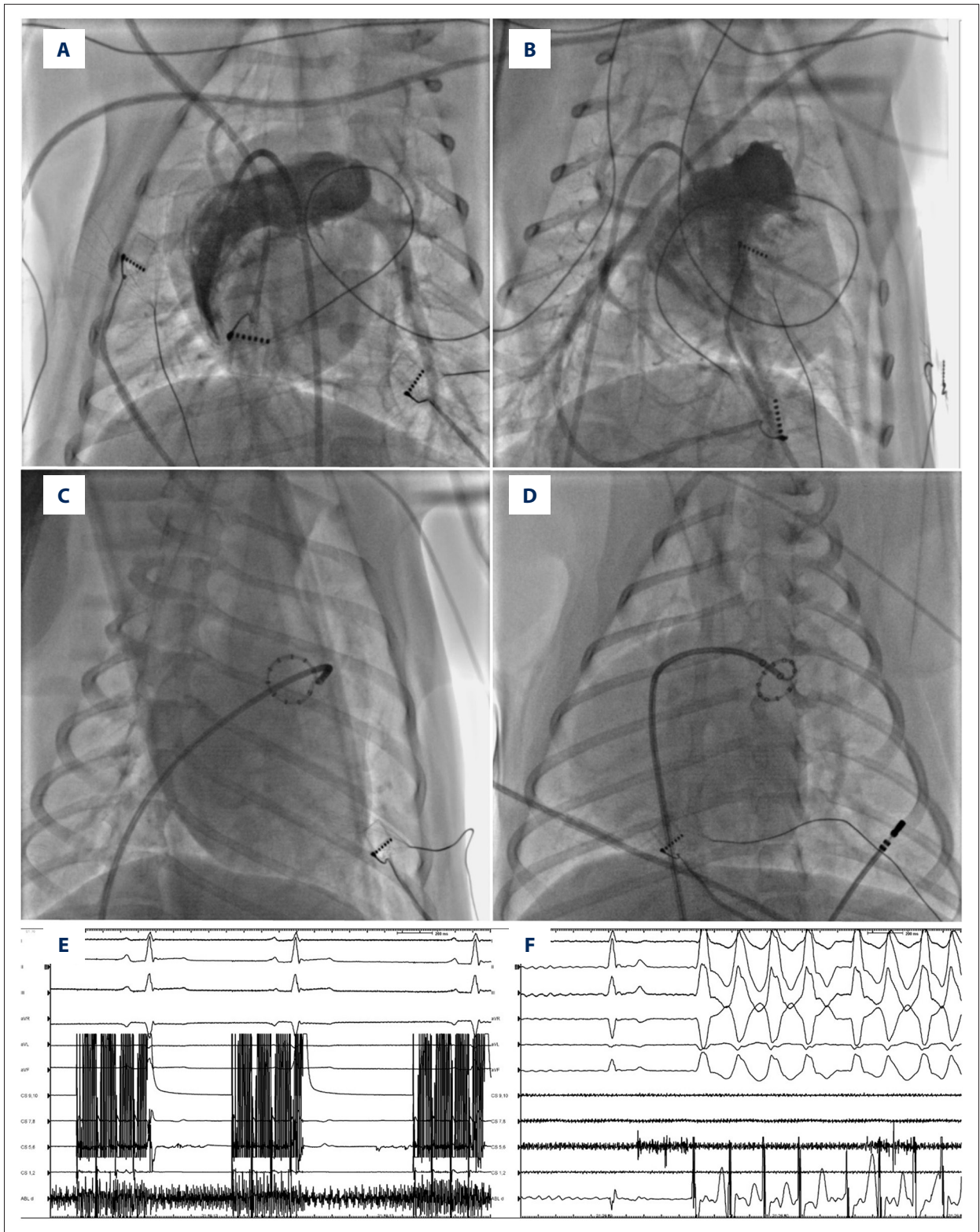


**Figure 1.** Biaxial images of right ventriculography in dogs (A, B). A lasso catheter was introduced into the pulmonary artery (C, D), and all the ventricular electrograms disappeared (E). High-frequency stimulation at 100 Hz (2-ms pulse duration) was applied to the catheter (E), and ventricular tachycardia exhibiting a left bundle branch block morphology and inferior axis was induced (F).

analyses. The distribution of the sympathetic nerves in different parts of the myocardial extension was observed. Five slices were randomly selected in each site and the lengths of the myocardial extension were measured.

### RVOT sympathetic nerve density distribution

The sympathetic nerve density distribution in the RVOT and other parts of the myocardial tissue was detected by tyrosine hydroxylase (TH) staining and transmission electron microscopy (TEM) (JEM-1400, 830.10U3) [13]. In addition, the formation of sympathetic nerve endings and features of the RVOT myocardium and other parts were observed.

### Statistical analysis

Continuous variables are expressed as the mean±standard deviation, or median with interquartile range (IQR), depending on the normality of the distribution. Mann-Whitney U test for non-normal data. Comparisons of continuous variables were made using a 2-tailed Student's *t* test for normal data or the 2-tailed Mann-Whitney U test for non-normal data. Comparisons of categorical variables were made using Fisher's exact test. Statistical calculations were performed using SPSS 16.0 software (SPSS, Chicago, IL). A *P*-value <0.050 was considered statistically significant.

## Results

### Establishment of a model of RVOT-VA mediated by sympathetic nerves

Premature ventricular contractions and paroxysmal ventricular tachycardia were induced in the experimental group after high-frequency stimulation as indicated by ECGs, and an associated pattern of left bundle branch block, right axis deviation, and II, III, and aVF lead R one-way wave was observed. The control group had no such premature ventricular contractions or ventricular tachycardia (Figure 1).

### Voltage mapping of the RVOT

Three-dimensional images of the RVOT were taken in the sinus under the guidance of a CARTO system (Figure 2). The color display for the voltage on bipolar electrograms of the myocardium ranged from red (low voltage zone, amplitude <0.5 mV) to purple (high voltage zone, amplitude >1.5 mV). Intermediate colors indicated a transitional voltage zone (amplitudes 0.5–1.5 mV).

The results indicated that the width of the voltage transitional zone in the septal wall (median 10.2 mm; IQR 7.8–14.1) is

wider than that of the free wall (median 4.5 mm; IQR 2.9–7.4; *P*=0.004). However, the width of the voltage transition zone of the experimental and control groups was similar.

### Detection of the serum concentrations of neurotransmitters

Compared with the control group, the serum concentrations of norepinephrine (experimental group: 173.02±17.38 ng/l cf. control group 102.84±15.55 ng/l; *P*<0.001) and neuropeptide Y (experimental group: 74.72±12.65 ng/l cf. control group: 57.95±9.30 ng/l; *P*=0.026) were significantly increased after stimulation. Moreover, the acetylcholine (experimental group: 1.05±0.90 ug/ml cf. control group: 4.45±2.21 ug/ml; *P*=0.004) concentration was lower in dogs from the experimental group compared with that of the control group (Figure 3).

### Detection of canine RVOT muscle extension distribution

H&E staining of the myocardium of both groups showed that the myocardial extension in the septal wall was significantly longer than that of the free wall (4.6 mm; IQR 2.6 to 6.7 cf. 1.3 mm; IQR -0.1 to 3.1; *P*=0.002; Figure 4).

### Detection of RVOT sympathetic nerve density distribution

The TH staining density in the septal wall was significantly greater than that of the free wall of both groups (Figure 5): experimental group (134.52±28.72 vs. 72.38±19.84; *P*=0.001) and control group (82.92±20.81 vs. 50.64±21.92; *P*=0.025). However, if it was compared with the control group, the TH staining density at the septal wall of the experimental group was significantly greater (Table 1). Results of TEM showed that the sympathetic nerves contained electron-dense core granules. The distribution of sympathetic nerve activities was significantly higher at the pulmonary valve level and RVOT septal wall than in other parts (Figure 6).

## Discussion

### Muscle extension and voltage transition zone

In a previous report of the distribution of successful catheter ablation sites within the RVOT using a 3-dimensional electroanatomic mapping system, Yamashina et al. [14] demonstrated that 88.7% of the successful ablation sites were located in the transitional voltage zone. Moreover, previous animal and human [11,12] studies showed that myocardial extension into the pulmonary artery is ubiquitous. These extensions frequently serve as origins of presumed RVOT arrhythmias. In our study, we found that RVOT voltage mapping can provide useful information regarding the extension of the muscle, which

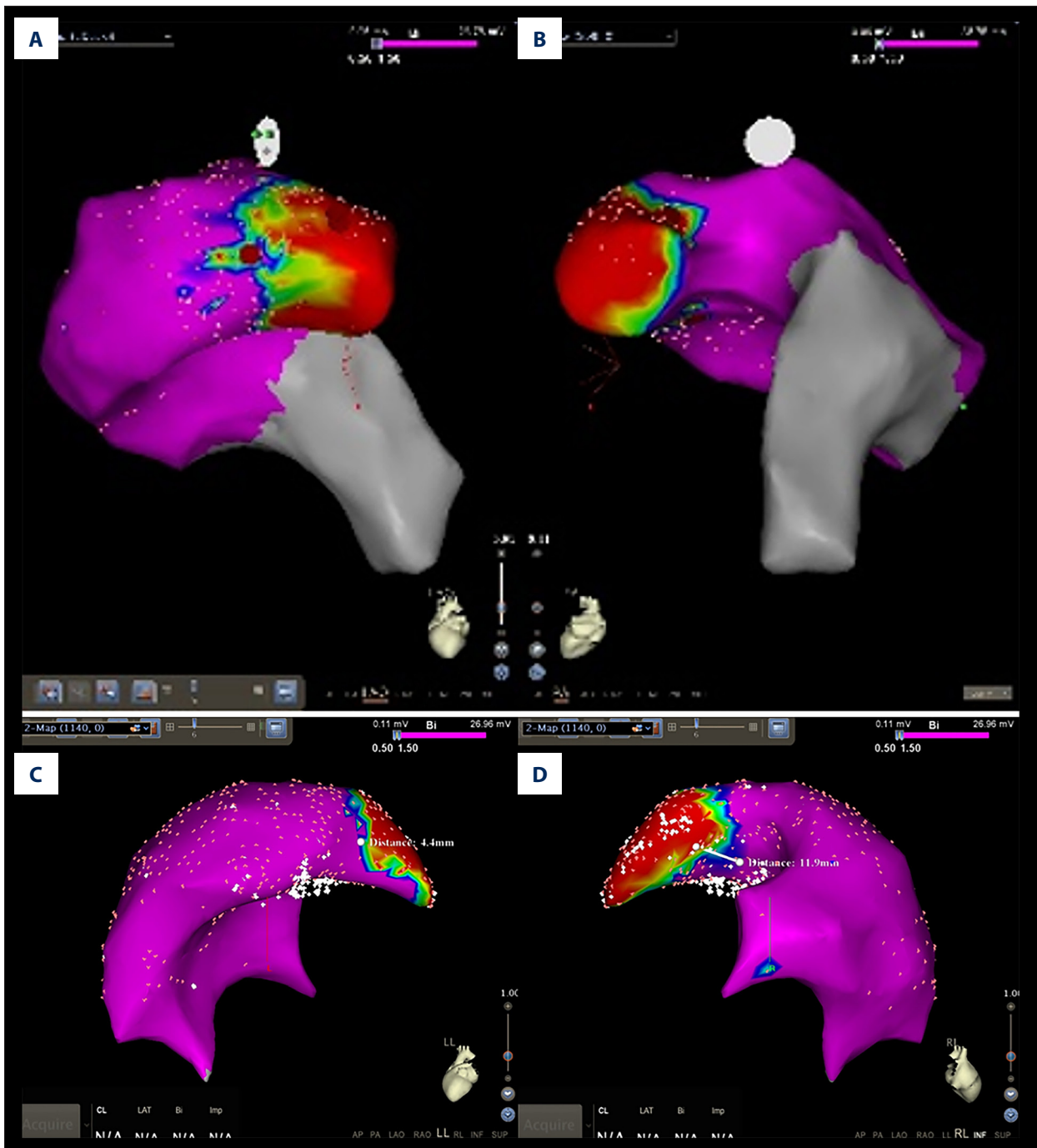


**Figure 2.** RVOT 3-dimensional conformation was taken in the sinus under the guidance of CARTO system. The color display for the voltage on bipolar electrograms of the myocardium ranged from red, representing the “low voltage zone” (amplitude  $<0.5$  mV), to purple, representing the “high voltage zone” (amplitude  $>1.5$  mV). Intermediate colors represented the “transitional voltage zone” (amplitudes between 0.5 and 1.5 mV) (A, B). The results showed that the width of the voltage transitional zone in the septal wall (D) is wider than that of the free wall (C).

positively correlated with the voltage transitional zone. Based on the above findings, we propose that the transitional voltage zone represents such a heterogeneously distributed arrhythmogenic myocardium around the pulmonary valve, which may

function as substrate for the pathogenesis of RVOT-VA in some patients. These findings may be helpful for the clinical localization of the ablation target region for patients with RVOT-VA

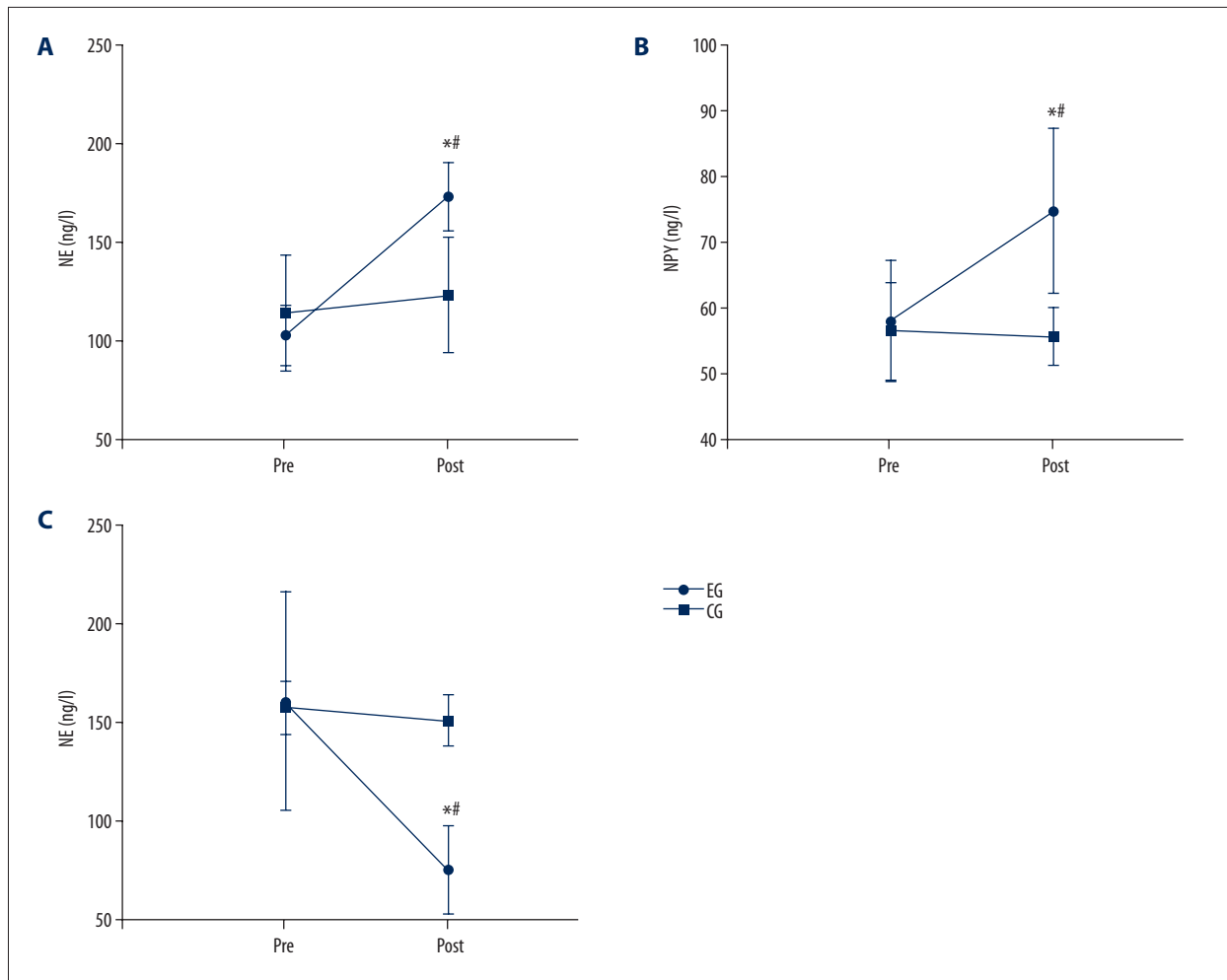


**Figure 3.** Compared with the control group (CG), the serum concentration of norepinephrine and neuropeptide Y in the experimental group (EG) were significantly higher after stimulation, and the acetylcholine concentration was significantly lower. \* Indicates that the neurotransmitter concentration changed significantly in the experimental group before and after stimulation,  $P < 0.05$ . # Indicates that the neurotransmitter concentration changed significantly, compared with the control group,  $P < 0.05$ .

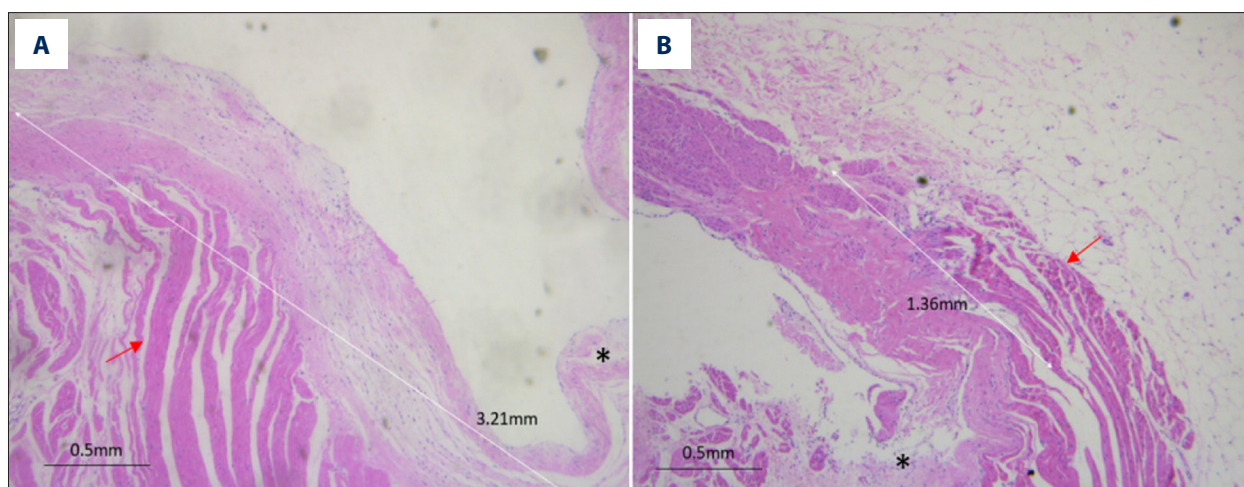


**Figure 4.** H&E staining showed that the myocardial extension in the septal wall (A) was longer than that in the free wall (B). \* Indicates the pulmonary artery valve, while the red arrows indicate muscle extension.

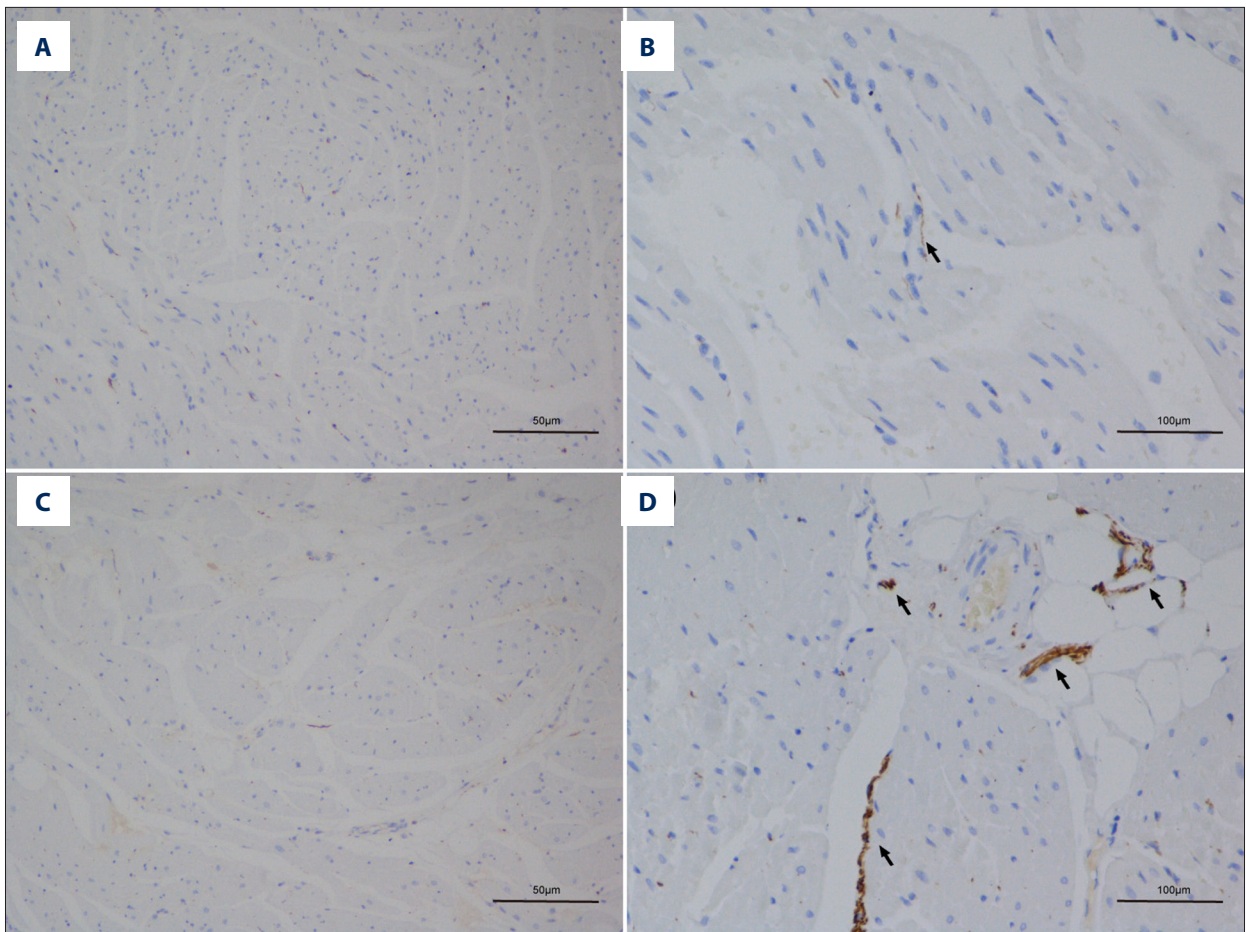


**Figure 5.** TH staining showed that the sympathetic nerve density in the septal wall (C, D) was higher than that in the free wall (A, B) of the RVOT; the brown-stained fibers indicate the sympathetic nerve (black arrows).

**Table 1.** TH density in different parts of the RVOT,  $\mu\text{m}^2/\text{mm}^2$ .

	Sample, n	Septal wall of RVOT	Free wall of RVOT
Control	6	82.92±20.81*	50.64±21.92
Experimental	6	134.52±28.72*#	72.38±19.84

\* Indicates that the sympathetic nerve density in the septal wall was significantly higher than that of the free wall,  $P<0.05$ ; # Indicates that the sympathetic nerve density in the experimental group was significantly higher than that of the control group,  $P<0.05$ .

### Sympathetic nerve and myocardial extension

It has been suggested that RVOT-VA may be caused by a triggered activity, possibly via cyclic adenosine monophosphate-mediated mechanisms [15–18]. However, this hypothesis was not adequate for explaining why RVOT-VA usually arises from a small discrete focus. Our H&E staining results showed that myocardial extension in the septal wall was longer than that in the free wall. Interestingly, a clinical trial also found that myocardial extension into the pulmonary artery in humans is ubiquitous [12]. These extensions frequently serve as origins of presumed RVOT arrhythmias. Therefore, it could be imagined

that changes in sympathetic nerves may affect the activity of myocardial extension and subsequently induce VA.

### VA and sympathetic nerves

Previous findings from a number of studies have also shown that the development of idiopathic VA may be associated with sympathetic nerve activation [6–8]. The middle cervical ganglia and the stellate ganglia have been shown to regulate the sympathetic aspect of cardiac physiology. One of the major sympathetic nerves (the ventromedial cardiac nerve) from the middle cervical and stellate ganglia traverses over the left

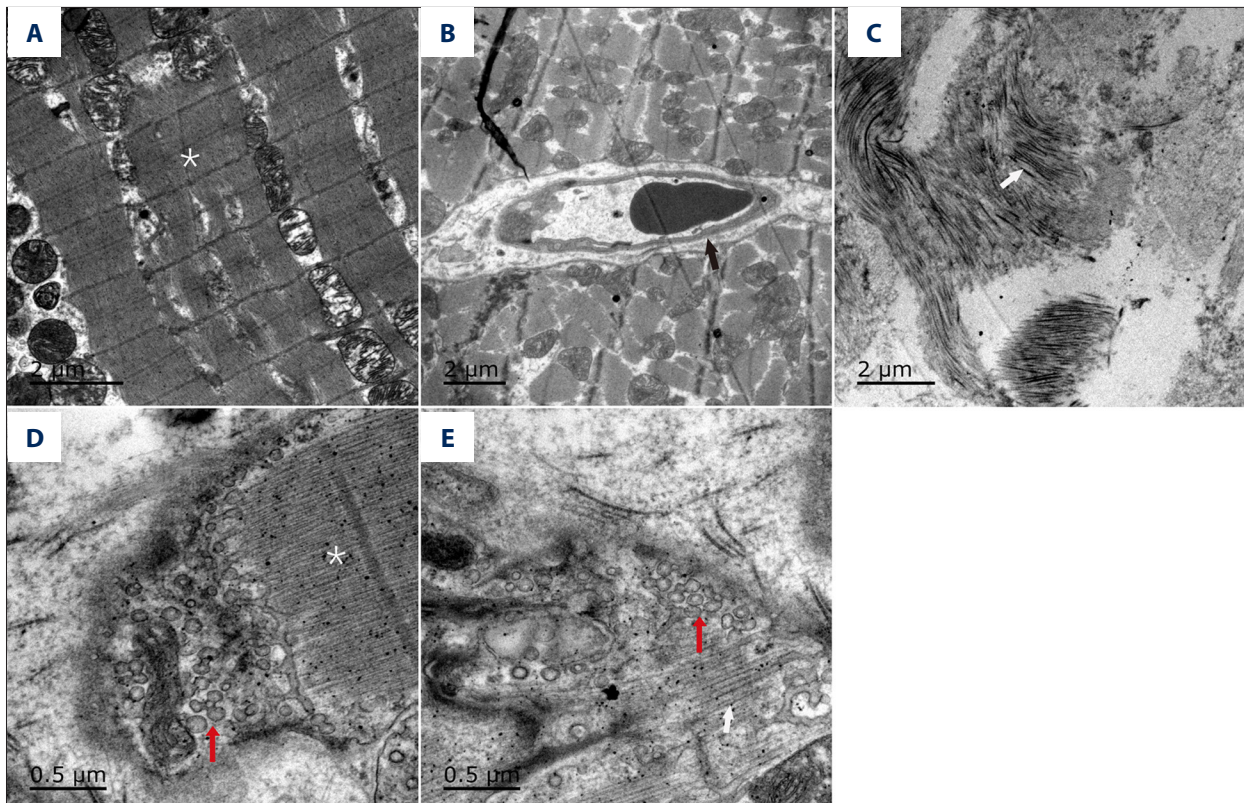


**Figure 6.** TEM of the different parts of the RVOT. No concomitant nerves beneath the pulmonary artery valve were detected (A, B). The black arrow indicates a capillary (B). The white arrow shows collagen fibers in the middle of the pulmonary artery (C). At the pulmonary valve level (D, E), the red arrows indicate sympathetic nerve terminals and a synaptic vesicle bubble.

pulmonary artery before innervating the proximal pulmonary artery and the RVOT [19]. According to the TH staining results of the present study, sympathetic nerve terminals were mostly distributed at the level of the pulmonary valve. In addition, the sympathetic nerve density in the septal wall was much higher than that of the free wall. Correspondingly, results of some clinical studies have also shown that 80% of idiopathic RVOT-VA originates from the septal wall. In this regard, it is possible that a hyperactive state of local sympathetic nerves may induce idiopathic VA in patients. In fact, it has been proposed that sympathetic nerve sprouting may be associated with the occurrence and prognosis of idiopathic arrhythmia. In our study, the sympathetic nerve density at the septal wall of the experimental group was significantly higher than that of the control group. These findings indicate that VA may induce local sympathetic nerve remodeling, which may be an important mechanism that triggers arrhythmia and maintains it.

### Study limitations

First, in the present study, mapping of the origin of the ectopy and tachycardia was not performed. Although we induced VA, which exhibited a left bundle branch block morphology and inferior axis, the exact site where the ectopy or tachycardia arose

was not investigated. Therefore, additional studies are required to confirm the origin of the VAs. Moreover, although we found that changes of the sympathetic nerves affected the activity of muscle extension and induced VA, it remains unclear how sympathetic nerve terminals affect muscle extension activity and induce VA. Since changes in calcium channel signaling and ryanodine receptor systems have been shown to be involved in the pathogenesis of many arrhythmias [20,21], we will evaluate calcium signaling and levels of the ryanodine receptor in the RVOT in future studies. Moreover, at this stage, we hypothesize that sympathetic nerve remodeling may result in increased calcium signaling events in myocardial extension and induce idiopathic VA.

### Conclusions

In this study, we established a canine model of VA originating from the RVOT mediated by sympathetic nerves. We found that stimulation of the pulmonary artery could activate local sympathetic nerves and enhance myocardial extension, which may be the foundation of RVOT-VA. Particularly, the RVOT voltage transitional zone was positively correlated with myocardial extension, which may serve as an important target for the catheter ablation of RVOT-VA clinically.



## References:

1. Nakagawa M, Takahashi N, Nobe S et al: Gender differences in various types of idiopathic ventricular tachycardia. *J Cardiovasc Electrophysiol*, 2002; 13: 633–38
2. Stevenson WG: Catheter ablation of monomorphic ventricular tachycardia. *Curr Opin Cardiol*, 2005; 20: 42–47
3. Lerman BB, Stein KM, Markowitz SM: Idiopathic right ventricular outflow tract tachycardia: a clinical approach. *Pacing Clin Electrophysiol*, 1996; 19: 2120–37
4. Badhwar N, Scheinman MM: Idiopathic ventricular tachycardia: Diagnosis and management. *Curr Probl Cardiol*, 2007; 32: 7–43
5. Volders PG: Novel insights into the role of the sympathetic nervous system in cardiac arrhythmogenesis. *Heart Rhythm*, 2010; 7: 1900–6
6. Hayashi H, Fujiki A, Tani M et al: Role of sympathovagal balance in the initiation of idiopathic ventricular tachycardia originating from right ventricular outflow tract. *Pacing Clin Electrophysiol*, 1997; 20: 2371–77
7. Kamakura S, Shimizu W, Matsuo K et al: Localization of optimal ablation site of idiopathic ventricular tachycardia from right and left ventricular outflow tract by body surface ECG. *Circulation*, 1998; 98: 1525–33
8. Zimmermann M: Sympathovagal balance prior to onset of repetitive monomorphic idiopathic ventricular tachycardia. *Pacing Clin Electrophysiol*, 2005; 28: S163–67
9. Zhou J, Scherlag BJ, Yamanashi W et al: Experimental model simulating right ventricular outflow tract tachycardia: A novel technique to initiate RVOT-VT. *J Cardiovasc Electrophysiol*, 2006; 17: 771–75
10. Jesuraj ML, Rao BH, Sharada K, Narasimhan C: Idiopathic right ventricular tract outflow tachycardia induced by high-frequency stimulation. *J Cardiovasc Electrophysiol*, 2013; 24: 221–23
11. Hasdemir C, Aktas S, Govsa F et al: Demonstration of ventricular myocardial extensions into the pulmonary artery and aorta beyond the ventriculo-arterial junction. *Pacing Clin Electrophysiol*, 2007; 30: 534–39
12. Liu CF, Cheung JW, Thomas G et al: Ubiquitous myocardial extensions into the pulmonary artery demonstrated by integrated intracardiac echocardiography and electroanatomic mapping: Changing the paradigm of idiopathic right ventricular outflow tract arrhythmias. *Circ Arrhythm Electrophysiol*. 2014 Aug;7(4):691-700
13. Felten S, Olschowka J: Noradrenergic sympathetic innervation of the spleen: II. Tyrosine hydroxylase (TH)-positive nerve terminals form synapticlike contacts on lymphocytes in the splenic white pulp. *J Neurosci Res*, 1987; 18: 37–48
14. Yamashina Y, Yagi T, Namekawa A et al: Distribution of successful ablation sites of idiopathic right ventricular outflow tract tachycardia. *Pacing Clin Electrophysiol*, 2009; 32: 727–33
15. Lerman BB, Stein K, Engelstein ED et al: Mechanism of repetitive monomorphic ventricular tachycardia. *Circulation*, 1995; 92: 421–29
16. Mont L, Seixas T, Brugada P et al: Clinical and electrophysiologic characteristics of exercise-related idiopathic ventricular tachycardia. *Am J Cardiol*, 1991; 68: 897–900
17. Kim RJ, Iwai S, Markowitz SM et al: Clinical and electrophysiological spectrum of idiopathic ventricular outflow tract arrhythmias. *J Am Coll Cardiol*, 2007; 49: 2035–43
18. Iwai S, Cantillon DJ, Kim RJ et al: Right and left ventricular outflow tract tachycardias: evidence for a common electrophysiologic mechanism. *J Cardiovasc Electrophysiol*, 2006; 17: 1052–58
19. Ito M, Zipes DP: Efferent sympathetic and vagal innervation of the canine right ventricle. *Circulation*, 1994; 90: 1459–68
20. Mackrill JJ: Ryanodine receptor calcium channels and their partners as drug targets. *Biochem Pharmacol*, 2010; 79: 1535–43
21. Wagner S, Maier LS, Bers DM: Role of sodium and calcium dysregulation in tachyarrhythmias in sudden cardiac death. *Circ Res*, 2015; 116: 1956–70